Wiley
Journal of Advanced Transportation
Volume 2024, Article ID 3582046, 14 pages
https://doi.org/10.1155/2024/3582046

WILEY

Research Article

Assessing the Effects of Interchange Warning Systems on Driving Risk: A Driving Simulator Study

Jingyang Li,[1,2] **Fengxiang Guo**,[1] **Wei Li**,[2] **Tianxiang Xiao**,[3] **and Chengyu Hu**[2]

[1]*Faculty of Transportation Engineering, Kunming University of Science and Technology, Kunming 650500, China*
[2]*National Engineering Research Center for Efficient Maintenance, Safety and Durability of Roads and Bridges, Broadvision Engineering Consultants Co., Ltd., Kunming 650041, China*
[3]*Yunnan Tenglong Freeway Co., Ltd., Dehong 678499, China*

Correspondence should be addressed to Wei Li; liwei@stwip.com

Received 13 December 2023; Revised 21 March 2024; Accepted 2 May 2024; Published 27 May 2024

Academic Editor: Arkatkar Shriniwas

To investigate the effects of proactive safety control systems suitable for highway interchanges and improve road traffic safety. Simulated driving experiments were conducted to test the effects of the interchange warning system (IWS) on the ramp, merging section, diverging section, and accident section. Random forest (RF) and SHapley Additive exPlanations (SHAP) are used to analyze the effects between driving behavior and driving risk change in both situations without and with IWS. The results show that (1) as driving risk increases, drivers tend to increase the frequency of braking and engage in more comprehensive saccade behaviors. Concurrently, there is an increase in acceleration and speed variation, leading to a gradual decrease in speed. (2) Compared with the SVR and XGBoost, RF can better fit the nonlinear relationship between driving risk and driver behavior characteristics with the application of IWS. (3) The IWS mainly reduces driving risk by affecting operation behavior. When the mean speed, speed standard deviation (SD), acceleration SD, and maximum braking depth are at 40 to 70 km/h, 3 to 10 km/h, 0 to 0.6 m/s^2, and 14 to 16, respectively, there is a significant reduction in driving risk. The application of the IWS expands the effective range of mean speed and speed SD for reducing driving risk to 40 to 100 km/h and 3 to 15 km/h, respectively.

1. Introduction

The driving environment and traffic flow in the interchange area of highways are more complex than other road sections. The longitudinal and lateral vehicles in the intertwined area lack coordination [1], resulting in significant differences in vehicle speeds and frequent lane changes [2]. Therefore, interchanges have become bottleneck areas that restrict the operational efficiency and safety of highways, representing high-risk road sections where conflicts and collisions are likely to occur [3, 4]. Research indicates that the occurrence of accidents is influenced by factors such as vehicle speed, traffic flow, driver characteristics, and road geometry. In weaving and merging areas, there is a higher likelihood of injuries and fatal accidents, while side-impact collisions are more common in merging and diverging sections. Additionally, rear-end collisions are more likely to occur in merging and overlapping areas [5, 6]. Existing studies have confirmed that comprehensive speed limit measures on highways can effectively reduce the severity of accidents and improve the overall traffic flow. However, relying solely on speed control measures is insufficient to significantly reduce the overall number of accidents [7, 8]. Implementing proactive warning and control systems can enhance the safety of interchange areas. These warning systems primarily include active lighting devices, dynamic information dissemination, and dynamic speed limit warning systems. Research on the impact mechanism between proactive warning and control methods and driver behavior characteristics and driving risk is crucial for reducing driving risk at interchanges and optimizing proactive warning and control systems.

In 1970, Inoue et al. [9] first proposed a highway warning system based on roadside equipment to detect road conditions and weather and to issue warning information to

drivers. Mahmud et al. conducted research on the layout and design of dynamic message signs in the warning system. Mahmud et al. [10, 11] analyzed the effects of dynamic message signs at different positions on curves with radius and investigated the effects of dynamic message sign borders, display text size, and roadside placement distance on the warning system. Gates et al. [12] studied the influence of different placement distances and display content on various vehicle types while Cui et al. [13] classified the collision risk on-ramps based on the analysis of vehicle trajectories and collision risk and guided drivers to pass through the ramps in an orderly manner by issuing information on the message board. In addition, researchers have devised ramp warning methods based on cooperative vehicle infrastructure system (CVIS). You et al. [14] categorized the CVIS into four modules: information collection, cooperative control, safety warnings, and evaluation. By using specific algorithms, they calculate the traffic volume and delay data of the main road and ramps and disseminate safety warning information for highway merging areas. Zhou et al. [15] proposed an active vehicle dynamic speed limit method for on-ramps. This method utilizes real-time perception of traffic conditions on the on-ramp through a vehicle-road coordination system. Based on the microscopic METANET model and ALINEA algorithm, a variable speed control strategy is designed to achieve dynamic control of vehicle speed. Wang et al. [16] employed a combination of various traffic sensors to collect real-time traffic status data in the merge area. Through the decision-making unit, the traffic status data is processed, analyzed, and updated periodically. A safety control warning is issued in real time through the vehicle-road coordination and display screen. Fang et al. [17] proposed a vehicle-side-roadside cooperative traffic guidance system for highways. Real-time perception of traffic conditions on the main highway and on-ramp is achieved through the roadside unit, enabling dynamic control of vehicle speed. Liu et al. [18] analyzed the key technical parameters of roadside unit (RSU) and the digital measurable image (DMI) method in the context of the CVIS and proposed an RSU deployment scheme based on DMI data to provide safety guidance for vehicles. Yang et al. [19], based on the process characteristics of vehicles approaching the merge area, designed an on-ramp speed control method that considers both driving time and risk of collision. Liu et al. [20] used vehicle-mounted ad-hoc network (VANET) to quickly forecast traffic accidents to rear vehicles and analyze road vehicle information in real time to help rear vehicles make reasonable emergency measures in time. While ample research has been conducted on the design and application of active safety control systems, there is a lack of comprehensive analysis on the impact of proactive warning and control methods on driver behavior and driving risk.

Therefore, this research takes the interchange warning system (IWS) deployed in Tenglong Expressway interchange in Yunnan Province as an example. It establishes the IWS based on random forest (RF) to model the impact of driver behavior characteristics and driving risk and combines the SHapley Additive exPlanations (SHAP) attribution analysis method to investigate the influence mechanism of driver behavior characteristics and driving risk under two scenarios: with and without warning systems. Identifying the significant influencing features of the IWS will provide reference for the design and optimization of proactive safety control systems.

2. Experiment

2.1. Experimental Design. The experiment researches the IWS deployed at the Tenglong Expressway interchange section in Yunnan Province, and the system sets up roadside unit (RSU) every 20 meters along the way. When a vehicle passes by, the signals from the RSU are transmitted to the system controller, which then coordinates the flashing of all the RSU in the area to monitor and warn drivers of potential hazards. The flashing pattern is as follows:

(1) Trail Display: upon detecting a vehicle, three RSUs behind the vehicle flash in red and form a trail, with a frequency of 60 flashes per minute

(2) Merge and Diverge Warning: when a vehicle enters or exits the on-ramp, RSUs within a range of 150 meters after the merged point or diverged point flash in red, with a frequency of 60 flashes per minute

(3) Accident Alert: in the event of accident detection, RSUs flash within a range of 200 meters behind the accident location in red, with a frequency of 60 flashes per minute

Based on the DSR-1000TS2.0 driver simulation platform independently developed by Kunming University of Science and Technology (Figure 1) and the VS-Design software for three-dimensional scene design, an experimental driving simulation route was constructed, consisting of four scenarios (Table 1): general ramp section (200 m), interchange merging section (250 m), interchange diverging section (250 m), and ramp accident section (200 m). Each scenario was applied both with and without IWS, resulting in a total of 8 roadway segments.

2.2. Experimental Procedure. The driving simulation experiment recruited a total of 50 drivers (average age 35, SD = 8.776, 15 females, 35 males). Each driver was required to wear an ErgoLAB psychophysiological instrument and an iView ETG2W eye tracker while driving through 8 experimental sections. Upon completion, the drivers followed the instructions of the staff to brake, turn off the engine, and fill out a subjective questionnaire on driving risk. The experimental process is depicted in Figure 2.

The experiment excluded 6 drivers who experienced dizziness or had abnormal data collection from the equipment. Eventually, a total of 44 drivers were identified as valid participants. This research utilizes expected variance, target confidence level, and margin of error to validate the adequacy of sample size [21], as shown in the following equation:

$$N = \frac{Z^2\sigma^2}{E^2}, \tag{1}$$

where N is sample size, Z is standard normal distribution statistic, σ is standard deviation, and E is maximum error.

To determine the minimum sample size, reflecting an unknown parameter at a 90% confidence level with a 10% significance level, Z is set at 1.25 and the range is taken as 0.25 to 0.5, with E being 10% [22]. In this study, σ is taken as 0.4, and the calculated value of N is 25. Thus, the sample size of the test drivers can be considered reasonable.

Each scenario segment on the road was considered as an analytical unit. A total of 352 segments of valid data were extracted, representing driving conditions with and without IWS in four different scenarios. The data were collected using a driving simulator, ErgoLAB psychophysiological instrument, and iView ETG2W eye tracker, and the collection indicators are shown in Table 2.

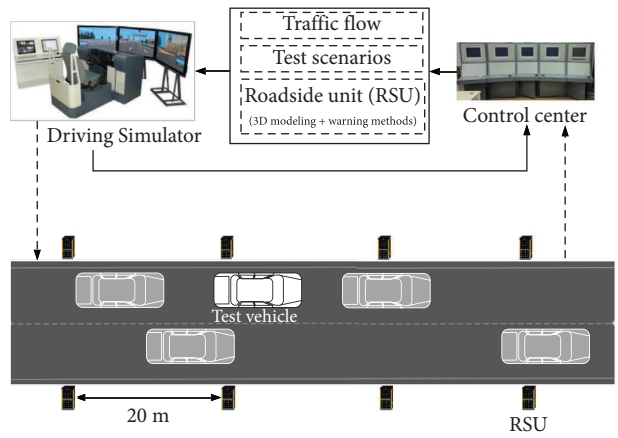

Figure 1: Test platform and structure.

3. Methods

3.1. Evaluation Framework. The research adopts driving safety as the guiding principle, selecting driver operational indicators, physiopsychological behavioral indicators, and eye movement behavioral indicators. It utilizes the fuzzy comprehensive evaluation method (FCE) to calculate the comprehensive scores of different drivers' driving risk, and an independent sample t-test was used to extract risk features influenced by the IWS and employs random forest (RF) combined with SHapley Additive exPlanations (SHAP) attribution analysis to elucidate the impact mechanism of the IWS on driving risk. This establishes a comprehensive evaluation framework (Figure 3) for the effectiveness of the IWS.

3.2. Data and Processing. The effectiveness of the IWS is influenced by the degree of risk in the scenarios. Due to the complexity of the road traffic environment, its effectiveness is affected by the conflict form, road alignment, and traffic flow, resulting in it being difficult to have a linear relationship with driving risk. To objectively evaluate the effectiveness of the IWS under different scenarios, the fuzzy comprehensive evaluation (FCE) method is employed to analyze the performance of drivers in different scenarios and partition driving risk [21].

3.2.1. Driving Risk Analysis. Vehicle speed and acceleration, brake pedal depth, heart rate, electrodermal activity, saccade velocity, and saccade amplitude were selected as the evaluation indicator set. These are used to characterize driver operating characteristics, physiological and psychological characteristics, and eye movement behavior characteristics, which reflect the driver's micro-operation process during driving, control of the vehicle, alertness level, and ability to obtain information through eye movements, make decisions, and take action.

The subjective questionnaire on driving risk categorizes driving risk into five levels, with higher levels indicating greater risk in a given scenario. To avoid discrepancies between drivers' subjective perceptions and their driving performance affecting the classification of indicators, the data are normalized, and the K-means clustering algorithm is applied to cluster the evaluation indicators. The evaluation indicators define five levels of evaluation comments, denoted as $U = \{u_1, u_2, u_3, u_4, u_5\}$. Since the clustering algorithm only provides the clustering categories without explaining the meaning of each category, an analysis of the clustering results is necessary. By combining the results of the subjective questionnaire on driving risk, the corresponding evaluation comment levels for each indicator range are comprehensively determined. For example, in the driving performance of category B (Table 3), the vehicle speed is relatively faster compared to other categories, but the corresponding brake pedal depth, acceleration, heart rate, galvanic skin response, saccade speed, and saccade amplitude, as well as their respective variations, are relatively small. This indicates that in the driving process, this category has a lower level of tension compared to other categories, requiring less frequent saccade behavior. Simultaneously, it can maintain a relatively fast and smooth speed. Moreover, 57% of the subjective questionnaire results for the risk assessment of drivers in this category are at level 0, 26% at level 1, and 17% at level 2. The driving performance of this category aligns well with the subjective risk assessment of drivers. Therefore, category B is defined as level 0. The same method is applied to determine the evaluation levels for all categories, as shown in Table 3.

3.2.2. Results of FCE. Using the FCE to analyze the above evaluation indicators, we determine the affiliation degree r_{ij} of the evaluation level corresponding to evaluation criteria $U = \{u_1, u_2, u_3, \ldots, u_n,\}$, establish the affiliation matrix R constituted by the evaluation set, use the entropy weight method to determine the fuzzy set A of the weight collection of each evaluation index, and finally get the fuzzy from the formulas (2)–(4) evaluation vector B.

$$R = \begin{pmatrix} r_{11} & r_{12} & \cdots & r_{1n} \\ r_{21} & r_{22} & \cdots & r_{2n} \\ \vdots & \vdots & \vdots & \vdots \\ r_{n1} & r_{n2} & \cdots & r_{nm} \end{pmatrix}, \tag{2}$$

$$A = (a_1, a_2, \ldots, a_n), \tag{3}$$

Table 1: Simulation scenarios and working mode of IWS.

Scenario description	IWS function	Scenarios
Ramp section: the test vehicle traveled along the ramp	The vehicle was traveling along the ramp, the yellow light on the roadside inducer in front of the vehicle was flashing, and the three RSUs behind the vehicle were flashing red and following the vehicle to form a trail	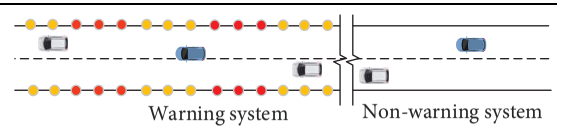
Merging section: test vehicles travel along the expressway and encounter vehicles merging from the ramp onto the expressway	No vehicles enter the expressway from the ramp, and the RSUs flash yellow lights. Vehicles enter the expressway, and the RSUs within a 150 m range of the expressway flash red lights, while the three RSUs behind the vehicle on the ramp flash red lights to form a trail	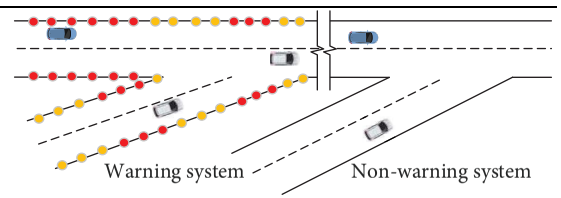
Diverging section: test vehicles travel along the expressway and encounter vehicles entering the ramp from the expressway	No vehicles enter the ramp from the expressway, and the RSUs flash yellow lights. Vehicles exit the mainline of the expressway, and the RSUs within a 150 m range of the mainline flash red lights, while the three RSUs behind the vehicle on the ramp flash red lights to form a trail	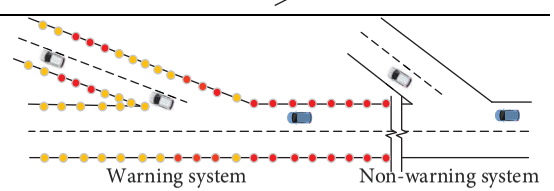
Ramp accident section: test vehicles encounter accident vehicles ahead while driving on the ramp	No traffic accidents on the ramp, and the RSUs flash yellow lights. When there is an accident on the ramp, the RSUs after the accident site flash red lights	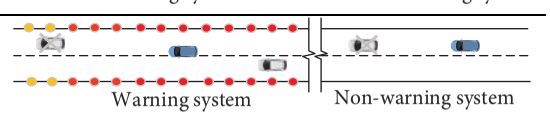

Symbol: RSUs (yellow), RSUs (red), test vehicle, other vehicle, accident.

(a) (b) (c)

Figure 2: Experimental procedure: (a) wearing instruments, (b) driving simulation experiment, and (c) example of scenario and RSU.

Table 2: Test data indicators.

Data	Indicator
Operational data	Speed (km/h), brake pedal depth, acceleration (m/s^2)
Physiopsychological data	Heart rate (beats/min), electrodermal activity (μS)
Eye movement data	Saccade amplitude (°), saccade velocity (°/s)

Note. The maximum value of the simulator brake pedal in this study was 20, and the value when the brake pedal was pressed to the limit position was calibrated to 20.

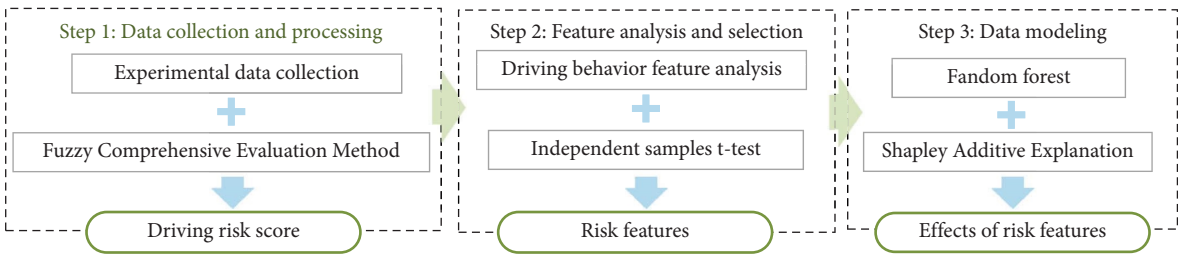

Figure 3: Comprehensive evaluation framework.

Table 3: Classification scope of evaluation indicators.

Clustering category	B	C	A	E	D
Risk level	0	1	2	3	4
Speed	(0.642, 0.812]	(0.332, 0.488]	(0.488, 0.642]	(0, 0.332]	(0.812, 1]
Brake pedal depth	(0, 0.243]	(0.243, 0.455]	(0.455, 0.559]	(0.559, 0.791]	(0.791, 1]
Acceleration	(0, 0.107]	(0.532, 0.671]	(0.315, 0.532]	(0.107, 0.315]	(0.671, 1]
Heart rate	(0, 0.122]	(0.122, 0.284]	(0.284, 0.488]	(0.488, 0.728]	(0.728, 1]
Electrodermal activity	(0, 0.071]	(0.071, 0.188]	(0.188, 0.442]	(0.442, 0.749]	(0.749, 1]
Saccade velocity	(0, 0.063]	(0.063, 0.124]	(0.124, 0.378]	(0.378, 0.698]	(0.698, 1]
Saccade amplitude	(0.252, 0.352]	(0.352, 0.412]	(0.412, 0.548]	(0, 0.252]	(0.548, 1]

$$B = A \circ R, \tag{4}$$

where A is the weights, R is the affiliation matrix, B is the fuzzy evaluation vector, and "$\circ$" is the weighted average type fuzzy operator fuzzy synthesis operator.

Using the FCE to analyze the driving risk, we define the score gradient matrix $V = (100, 80, 60, 40, 20)$ for the comment set $L = \{l_1, l_2, l_3, l_4, l_5\}$. The higher the driving risk, the lower the score, the multiplication of B and V is the composite score under each scenario. Subsequently, we calculate the comprehensive score for each driver and the mean score for all drivers. Table 4 shows the results of calculating the fuzzy evaluation vectors and composite scores for the first driver, while Table 5 shows the mean score for all drivers.

3.3. Feature Analysis and Selection

3.3.1. Feature Analysis. In order to visually analyze the relationship between driver's behavioral characteristics and driving risk, independent sample T-tests were used to analyze operation behavior characteristics, psychophysiological characteristics, and eye movement characteristics, respectively. The results of the independent samples T-test are shown in Table 6.

(1) Operation Behavior. The analysis of driver's operation characteristics can be seen in Figure 4. As the driving risk increases in different experimental scenarios, the changing trends of each indicator are basically consistent between the two cases with and without IWS. However, in the application of IWS, the increasing trend of acceleration SD, average

Table 4: Composite scores of driver#1 under different scenarios.

Scenarios	IWS application	Fuzzy evaluation vectors	Composite score
Ramp section (scenario 1)	Unapplied	(0.082, 0.236, 0.571, 0.049, 0.062)	64.54
	Applied	(0.100, 0.203, 0.613, 0.061, 0.023)	65.92
Merging section (scenario 2)	Unapplied	(0.101, 0.193, 0.488, 0.079, 0.139)	60.76
	Applied	(0.051, 0.158, 0.701, 0.049, 0.041)	62.52
Diverging section (scenario 3)	Unapplied	(0.217, 0.295, 0.332, 0.081, 0.075)	69.96
	Applied	(0.180, 0.336, 0.461, 0.017, 0.006)	73.34
Ramp accident section (scenario 4)	Unapplied	(0.039, 0.051, 0.584, 0.198, 0.127)	53.48
	Applied	(0.059, 0.091, 0.695, 0.066, 0.088)	59.28

Table 5: Mean score of all drivers under different scenarios.

Scenarios	IWS application	Mean score		Risk ranks
Ramp section (scenario 1)	Unapplied	65.00	66.46	L2
	Applied	67.92		
Merging section (scenario 2)	Unapplied	61.34	63.43	L3
	Applied	65.52		
Diverging section (scenario 3)	Unapplied	70.02	73.27	L1
	Applied	76.34		
Ramp accident section (scenario 4)	Unapplied	53.34	55.31	L4
	Applied	57.28		

Table 6: The results of the independent samples t-test.

Characteristics type	Characteristics	IWS	Scenario 1	Scenario 2	Scenario 3	Scenario 4
Operation behavior	Mean speed (km/h)	Unapplied	58.02	75.31	86.36	41.40
		Applied	57.62	64.33	64.15	50.45
		Sig	0.902	0.002**	0.000**	0.005**
	Speed SD (km/h)	Unapplied	0.64	0.81	0.35	1.60
		Applied	1.03	1.60	0.65	1.81
		Sig	0.017*	0.000**	0.042*	0.202
	Acceleration SD (m/s^2)	Unapplied	6.38	6.66	3.58	14.23
		Applied	7.88	11.18	7.83	16.15
		Sig	0.186	0.018*	0.001**	0.235
	Mean brake pedal depth	Unapplied	3.51	5.51	2.41	11.32
		Applied	6.02	10.10	3.03	10.87
		Sig	0.039*	0.009**	0.357	0.708
	Maximum brake pedal depth	Unapplied	0.27	0.83	0.22	0.94
		Applied	0.37	1.08	0.2	1.55
		Sig	0.376	0.047*	0.838	0.410*
	Brake pedal depth SD	Unapplied	0.82	1.64	0.40	2.60
		Applied	1.19	3.09	0.65	2.76
		Sig	0.232	0.015**	0.358	0.711
Psychophysiological characteristics	Heart rate SD	Unapplied	3.73	4.84	4.3	5.44
		Applied	4.69	4.22	3.99	5.07
		Sig	0.335	0.562	0.779	0.712
	Electrodermal activity (μS)	Unapplied	7.16	7.67	6.71	7.25
		Applied	7.08	7.21	7.49	8.08
		Sig	0.691	0.67	0.309	0.574
Eye movement characteristics	Mean saccade amplitude (°)	Unapplied	2.56	2.19	1.6	2.84
		Applied	2.58	2.56	2.14	2.20
		Sig	0.976	0.231	0.029*	0.265
	Mean saccade velocity (°/s)	Unapplied	64.67	72.16	53.61	72.84
		Applied	73.50	74.90	51.74	70.70
		Sig	0.045*	0.623	0.918	0.637

*Significant difference at 0.05 level. **Significant difference at 0.01 level.

depth of brake pedal, and brake pedal depth SD are larger than those without IWS, while the increasing trend of speed SD and maximum depth of brake pedal are smaller than those without IWS. The decrease in mean speed is also smaller than that without IWS. The acceleration SD of the vehicle (scenarios 1, 2, and 3; Sig = 0.017, 0.000, 0.042 < 0.05), speed SD (scenarios 2 and 3; Sig = 0.018, 0.001 < 0.05), maximum depth of brake pedal (scenarios 1 and 2; Sig = 0.039, 0.009 < 0.05), mean brake depth (scenarios 2 and 4; Sig = 0.047, 0.041 < 0.05), and brake depth SD (scenario 2, Sig. = 0.015 < 0.05) are all higher than those without IWS, and there are significant differences in different scenarios.

With the above analysis, as the driving risk increases, the driver will brake harder and more frequently to control the speed of the vehicle and try to keep the speed stable. Comparing the situation with and without IWS, the IWS can better guide the driver to brake and stabilize the vehicle speed to avoid potential risk.

(2) Psychophysiological Behavior. According to the psychophysiological characteristics analysis of driving, as shown in Figure 5, as the driving risk increases, both the heart rate SD and the mean electrodermal activity show an upward trend. When there is IWS, the degree of increase in the heart rate SD for drivers is weaker, while the mean electrodermal activity is the opposite. At the same time, the heart rate SD is generally lower, and the mean electrodermal activity is generally higher when there is IWS. However, the analysis shows no significant difference in drivers' psychophysiological behaviors with or without the IWS.

In summary, drivers tend to exhibit higher levels of tension, cognitive arousal, and vigilance as driving risk increases. Installing IWS is beneficial in reducing the level of driver tension as driving risk rises, while maintaining a high level of cognitive arousal and vigilance.

(3) Eye Movement Behavior. The analysis of the driver's eye movement characteristics depicted in Figure 6 reveals that there are varying degrees of upward trend in saccade amplitude and saccade speed as driving risk increases. In scenarios where driving risk is higher, the amplitude and velocity of saccades are lower when an IWS is applied than when it is unapplied. When an IWS is applied, the amplitude of saccades is more stable, and the velocity of saccades is faster. In addition, significant differences exist between scenarios with and without an IWS in scenario 3 (Sig. = 0.029 < 0.05) and scenario 1 (Sig. = 0.045 < 0.05).

Based on the above analysis, drivers tend to increase both the amplitude and velocity of their saccades in high-risk driving scenarios, allowing for faster acquisition of traffic information. When IWS is applied, drivers are able to maintain a wider and more stable amplitude of saccades, while also increasing their saccades velocity, enabling them to better identify potential road risk.

3.3.2. Feature Selection. The indicators showing significant differences between the application and without application of IWS in feature analysis, along with the comprehensive scores of all drivers in different scenarios, were selected to construct a risk feature dataset for modeling. This facilitated the analysis of the relationship between IWS, driver behavior characteristics, and driving risk. Details of the features' range and encoding can be found in Table 7.

3.4. Data Modeling. To investigate the impact of IWS on driver behavior and driving risk, we comprehensively evaluate the efficacy of IWS, establish a nonlinear model between the IWS, driver characteristics, and driving risk using the random forest regression algorithm (RF), and analyze the effectiveness of the IWS using the SHapley Additive exPlanations (SHAP).

3.4.1. Random Forest. The RF combines the Bagging ensemble algorithm and the decision tree algorithm. By incorporating randomness throughout the entire sampling process, it mitigates the issue of overfitting that decision trees face during growth. The CART regression tree branches at nodes based on the principle of minimizing the mean absolute error. For any variable K that needs to be branched, it is necessary to determine the variable and parent node that satisfy the minimum sum of mean absolute errors for the two datasets D_1 and D_2 divided by the corresponding parent nodes [23]. The corresponding formula is as follows:

$$\min_{K,s}\left[\min_{m_1}\sum_{x_i\in D_1(K,s)}\left|y_i-m_1\right|+\min_{m_2}\sum_{x_i\in D_2(K,s)}\left|y_i-m_2\right|\right], \tag{5}$$

where m_1 is the output mean value of D_1 subnode; m_2 is the output mean value of D_2 subnode; x_i is the input sample; y_i is the node output value.

3.4.2. Model Optimization and Evaluation. To prevent the RF model overfitting effectively and enhance its performance, this study employs an 80% data allocation for training and 20% for testing. Through grid search and ten-fold cross-validation, the model undergoes hyperparameter optimization. The ten-fold cross-validation divides the training set into 10 subsets for 10 training iterations, using 9 subsets for training and 1 subset for validation in each iteration, leading to the determination of the optimal model parameters. The error and optimal parameters for model training are shown in Figure 7 and Table 8, respectively.

To evaluate the accuracy and reliability of the RF model, the mean absolute error (*MAE*), mean squared error (*MSE*), and root mean squared error (*RMSE*) are used as metrics to evaluate the fit of the regression model. The definitions of these indicators are as follows:

$$MAE=\frac{1}{m}\sum_{i=1}^{m}\left|\left(y_i-\overline{y}_i\right)\right|, \tag{6}$$

$$MSE=\frac{1}{m}\sum_{i=1}^{m}\left(y_i-\overline{y}_i\right)^2, \tag{7}$$

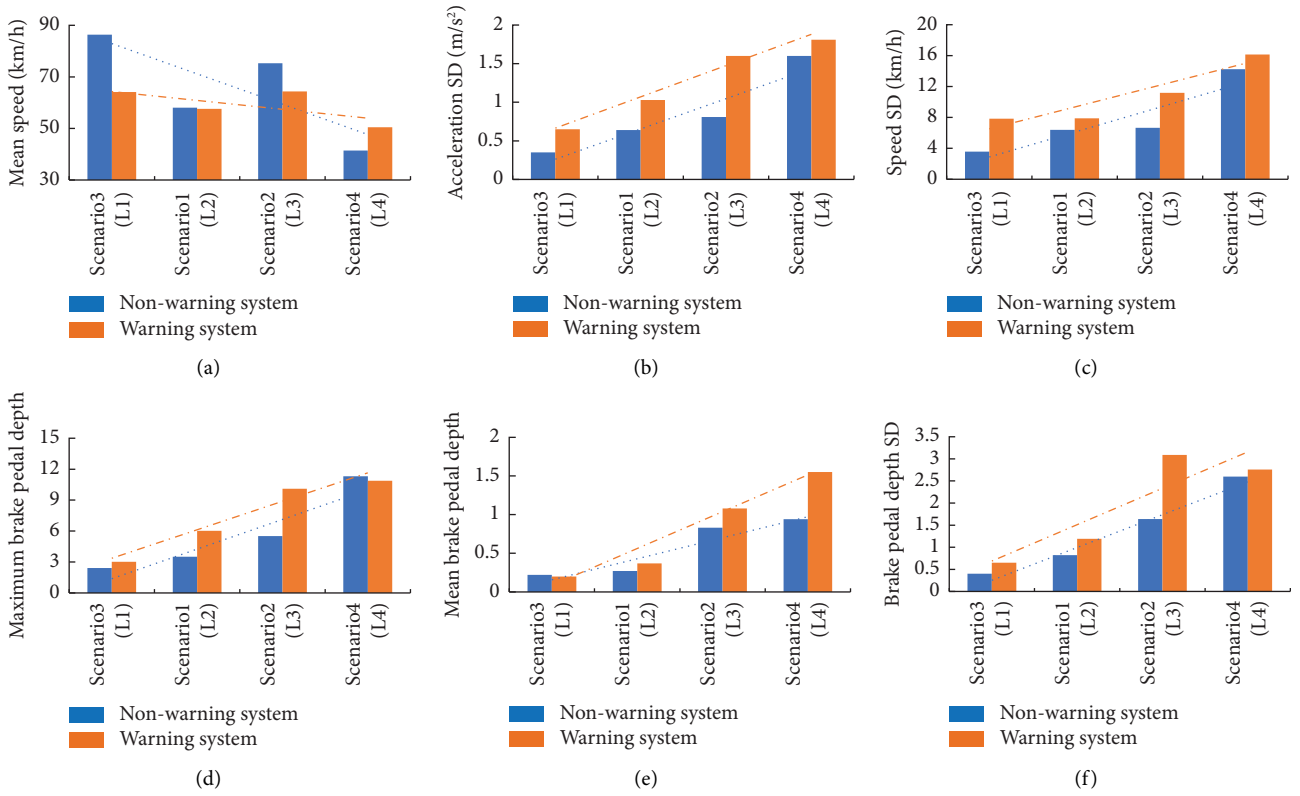

Figure 4: Operation behavior under different driving risk: (a) mean speed, (b) acceleration SD, (c) speed SD, (d) maximum brake pedal depth, (e) mean brake pedal depth, and (f) brake pedal depth SD.

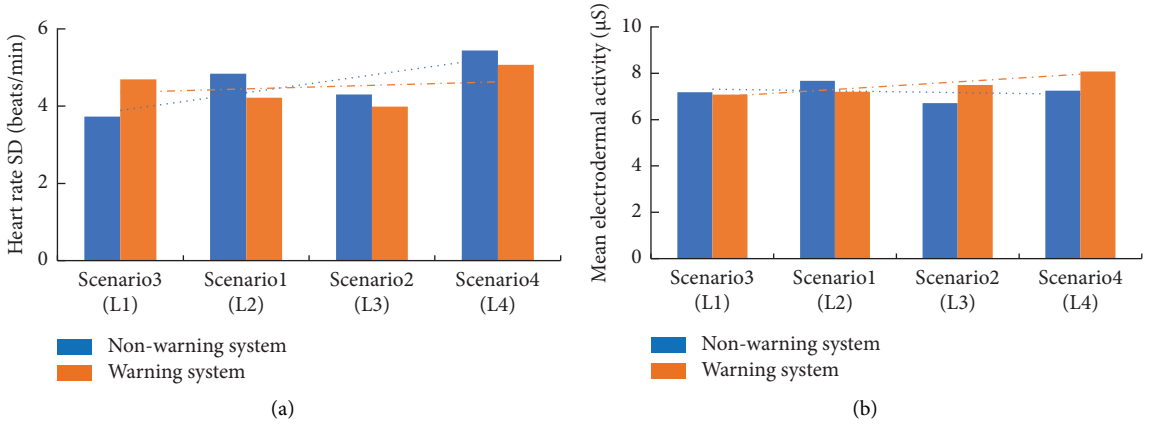

Figure 5: Psychophysiological behavior under different driving risk: (a) heart rate SD and (b) mean electrodermal activity.

$$RMSE = \sqrt{\frac{1}{m}\sum_{i=1}^{m}(y_i - \overline{y}_i)^2}, \tag{8}$$

where m is the total number of sample data; $\overline{y}_i$ and y_i are the predicted and observed values, respectively.

The performance comparison is conducted by SVR (support vector regression machine), XGBoost (extreme gradient boosting machine), and RF (random forest), respectively, and the calculated results of *MAE*, *MSE*, and *RMSE* of each model are shown in Table 9, and the RF has lower *MAE*, *MSE*, and *RMSE* compared with SVR and XGBoobt, which indicates that RF has a better fitting effect, which can better express the relationship between the IWS, driving behavior characteristics and driving risk, and can better resolve the mechanism of different variables on driving risk.

3.4.3. SHapley Additive exPlanations (SHAP). SHAP calculates the SHAP value by building an additive explanatory model, analyzing "contributions" of all features as to the target. The SHAP value is the degree of "contribution" assigned to each feature, providing an excellent explanation

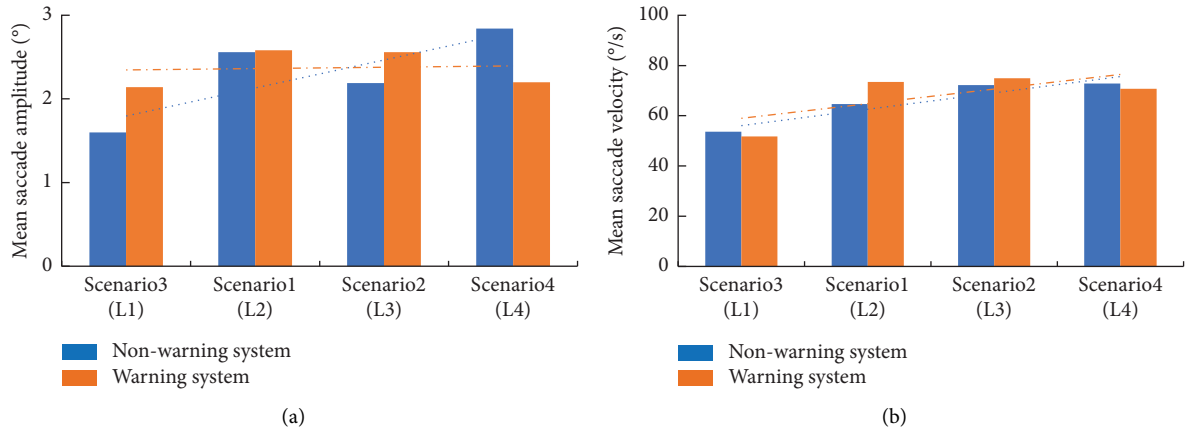

Figure 6: Eye movement behavior under different driving risk: (a) mean saccade amplitude and (b) mean saccade velocity (°/s).

Table 7: Classification and coding of risk features.

Feature categories		Features	Feature codes and range
Degree of risk		Driving risk	[42.4, 83.6]
IWS arrangements		IWS	0 = unapplied, 1 = applied
Driver behavioral characteristics	Operation behavior	Mean speed (km/h)	[24.82, 114.20]
		Speed SD (km/h)	[0.08, 44.9]
		Acceleration SD (m/s^2)	[0.01, 3.34]
		Mean brake pedal depth	[0, 10.26]
		Maximum brake pedal depth	[0, 20.00]
		Brake pedal depth SD	[0, 9.97]
	Eye movement behavior	Mean saccade amplitude (°)	[0, 8.45]
		Mean saccade velocity (°/s)	[0, 191.23]

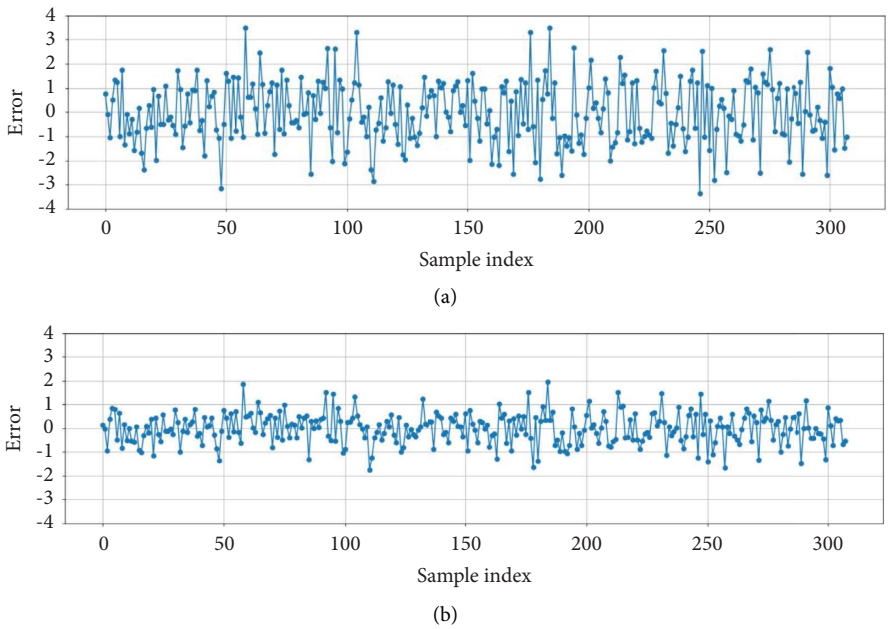

Figure 7: Error curve between true and predicted values: (a) before optimization and (b) after optimization.

Table 8: Optimal hyperparameters of RF model.

Hyperparameter	Range	Optimal value
n_estimators	[80, 300]	120
max_depth	[2, 7]	4

Table 9: Model evaluation indicator.

Models	MAE		MSE		RMSE	
	Train	Test	Train	Test	Train	Test
SVR	1.78	1.75	4.45	4.32	2.11	2.08
XGBoost	1.22	1.28	2.79	2.89	1.67	1.70
RF	0.51	0.54	0.86	0.81	0.92	0.90

for the mechanisms of both multivariate interactions and single variables [24]. In the research, the application of the IWS and driver behavioral characteristics is input as feature values, and the SHAP value is obtained based on their contribution to the driving risk, as shown in formulas (9) and (10):

$$f(x_i) \approx g(z_i') = \phi_0 + \sum_{j=1}^{N} \phi_{ij} z_{ij}', \tag{9}$$

where N represents the number of features, $z_{ij}' \in \{0,1\}^N$ represents the set of features belonging to the sample among N features, ϕ_j represents the contribution of feature i, and ϕ_0 represents the dummy contribution.

$$\phi_{ij} = \sum_{w \in x_i} \frac{(|s|-1)!\,(N-|s|)!}{N!} [f(s) - f(s - \{j\})], \tag{10}$$

where ϕ_{ij} represents the contribution of any variable, s is a subset of the set of variables, and $|s|$ represents the number of variables in the subset.

4. Results and Discussion

4.1. Importance of Risk Features. The contribution of different features to driving risk is shown in Figure 8(a), which illustrates the overall impact of each risk feature on driving risk and arranges them in descending order of their impact on driving risk. The two variables with a greater impact are the IWS and the speed SD, and the impact of mean speed and acceleration SD, mean saccade velocity, and amplitude on driving risk is roughly similar, while the remaining features have limited impact on driving risk. The influence of the IWS and driver behavioral characteristics on driving risk is obtained from the calculation of the SHAP value, and the positive and negative SHAP values represent the features' positive and negative impacts on risk level. As shown in Figure 8(b), it is evident that when the IWS value (0 = unapplied and 1 = applied) is higher, the corresponding SHAP value is negative, indicating that the IWS can reduce driving risk. Conversely, when the speed SD and acceleration SD are larger, the corresponding SHAP value is positive, signifying that higher speed and acceleration SD lead to increased driving risk.

4.2. Effects of Risk Features. The driver's behavioral characteristics are classified into two categories, without IWS and with IWS. The SHAP values are used for partial dependence analysis, aiming to investigate the impact mechanisms between driver behavior features and driving risk under the two different applications of IWS as illustrated in Figure 9. The vertical axis represents the SHAP values, while the horizontal axis indicates various driver behavior features.

(1) In Figure 9(a), the mean speed is concentrated within the range of 40 to 70 km/h, and the SHAP values are mostly below zero, suggesting that it reduces driving risk under both without and with IWS conditions. The mean speed is more scattered without IWS, particularly when it ranges from 0 to 40 km/h and from 70 to 100 km/h, the SHAP values are mostly above zero, indicating an increase in driving risk. However, with IWS, the mean speed concentrates within the range of 40 to 80 km/h, and the SHAP values are mostly below zero when the speed is between 70 and 100 km/h, indicating that there is still a reduction in driving risk. This demonstrates that controlling the average mean speed within the range of 40 to 70 km/h on interchange ramps can effectively mitigate driving risk. Furthermore, installing IWS concurrently can expand the range of mean speed at which risk can be mitigated and concentrate the mean speed more within the 40 to 80 km/h range.

(2) In Figure 9(b), when the speed SD is within the range of 3 to 10 km/h, the majority of SHAP values are below zero. This indicates a reduction in driving risk under both the conditions without and with IWS. When the speed SD exceeds 10 without IWS, the SHAP values are mostly above zero, resulting in an increase in driving risk. However, with IWS, the SHAP values are lower compared to the condition without IWS, indicating a weakening of the elevated impact of speed SD on driving risk. Simultaneously, the range where it has a reducing effect expands. In the range of 10 to 15 km/h, the majority of SHAP values remain below zero, indicating a reduction in driving risk for driving. Conversely, beyond 15 km/h, the majority of SHAP values are above zero, posing an increase in driving risk. This illustrates that within the range of 3 to

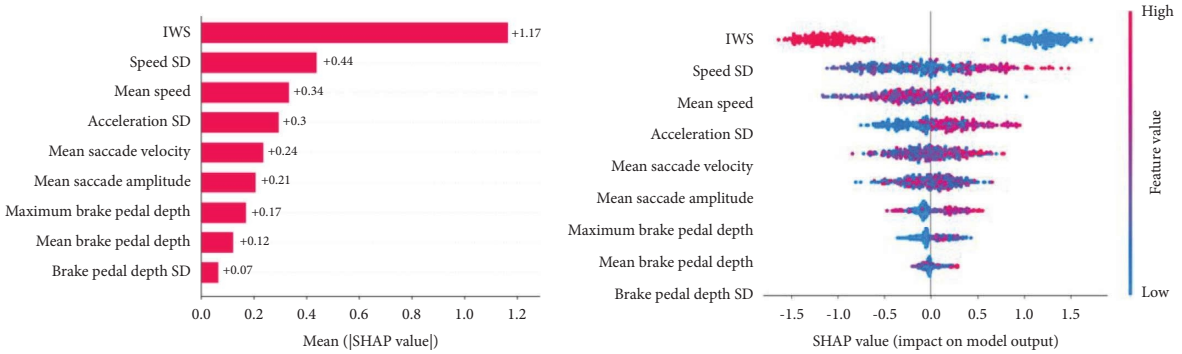

Figure 8: SHAP model analysis: (a) feature importance and (b) summary plot.

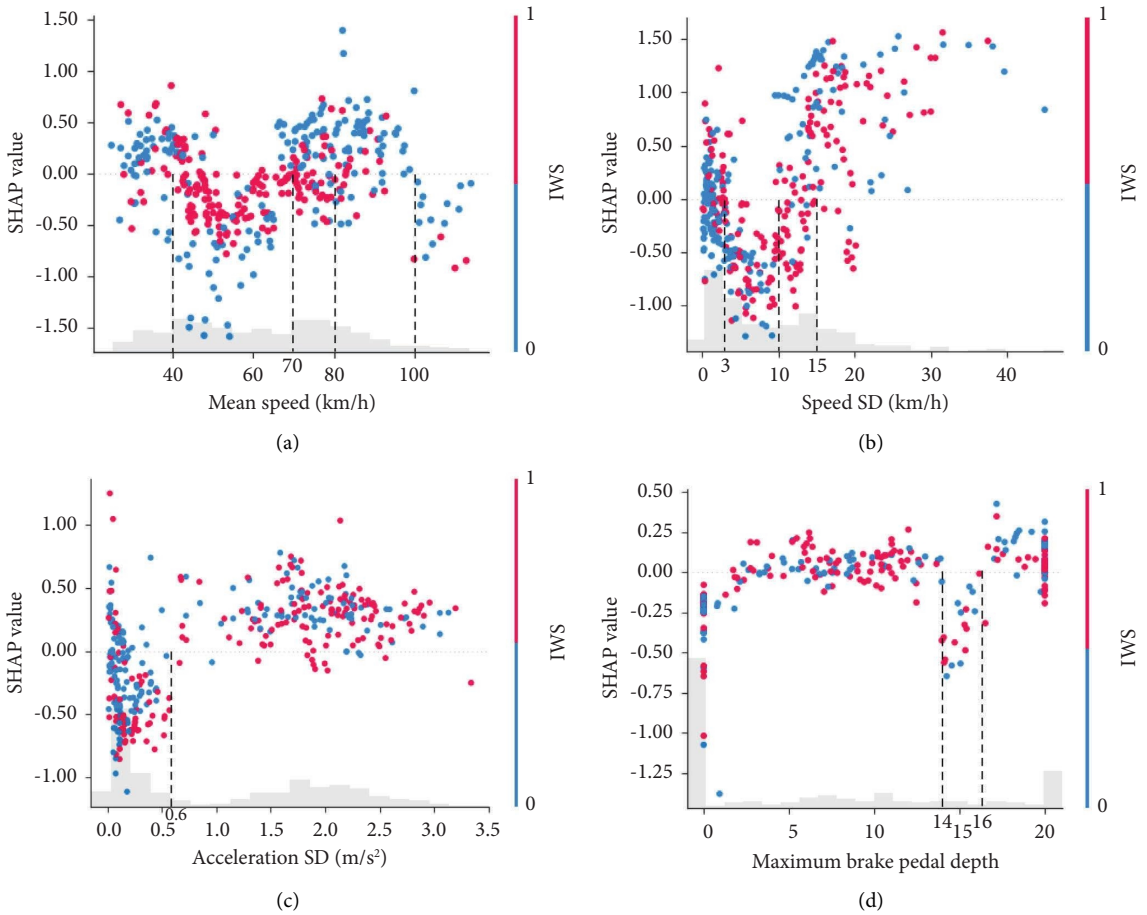

Figure 9: Continued.

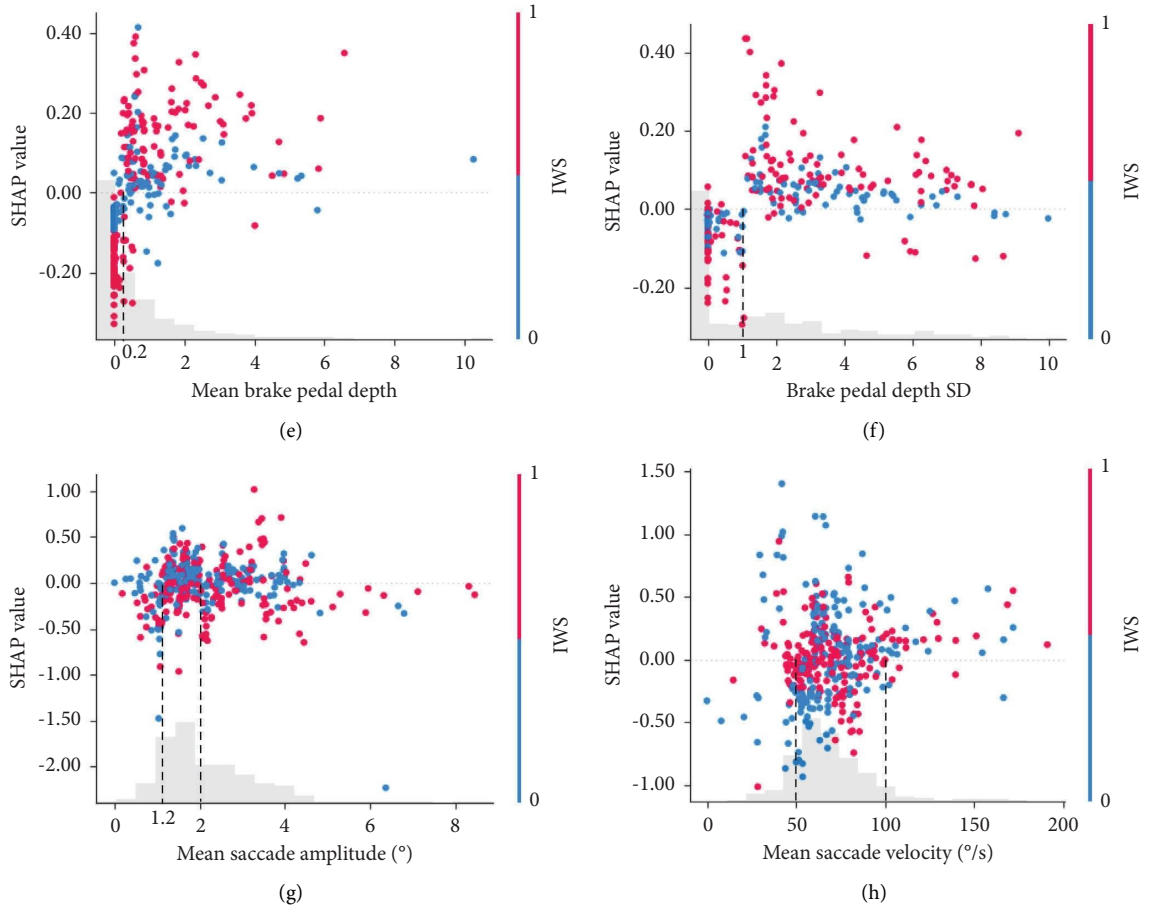

Figure 9: Analysis of SHAP value of driver behavior features: (a) mean speed, (b) speed SD, (c) acceleration SD, (d) maximum brake pedal depth, (e) mean brake pedal depth, (f) brake pedal depth SD, (g) mean saccade amplitude, and (h) mean saccade velocity.

10 km/h for the speed SD, driving risk can be reduced, and the application of IWS can extend the range of speed SD at which risk can be mitigated.

(3) In Figure 9(c), in both with and without IWS, the SHAP value is higher than 0 when the acceleration SD is greater than 0.6 m/s^2, indicating that the risk of driving is elevated in both conditions, and the SHAP value is lower than 0 when the acceleration SD is less than or equal to 0.6 m/s^2, indicating that there is a reduction of the risk in both conditions, but this reduction is more obvious compared to with the application of IWS. This indicates that driving is safer when the standard deviation of acceleration is 0 to 0.6 m/s^2, and the installation of IWS partially improves driving safety.

(4) In Figure 9(d), the SHAP values are below 0 and above 0 for the maximum braking depth ranges of 14 to 16 and 16 to 19, respectively, under the conditions with and without IWS. This indicates a reduction and an increase in driving risk, respectively. When the maximum braking depth is within the range of 1 to 14, there is no significant increase or decrease in risk. Hence, maintaining the maximum braking depth within the range of 14 to 16 can enhance driving safety. Furthermore, the installation of IWS has no significant impact on the maximum braking depth.

(5) In Figures 9(e) and 9(f), under the conditions of without and with IWS, when the mean brake pedal depth and brake pedal depth SD are in the ranges 0 to 0.2 and 0 to 1, respectively, the SHAP value is lower than 0, indicating a significant risk reduction. Conversely, when the mean brake pedal depth and brake pedal depth SD exceed 0.2 and 1, respectively, the SHAP value is higher than 0, indicating an increase in driving risk. Furthermore, the application of IWS has a weaker influence on the relationship between the mean brake pedal depth, brake pedal depth SD, and driving risk.

(6) In Figures 9(g) and 9(h), the distributions of SHAP values for mean saccade amplitude and mean saccade velocity are not significantly different under both without and with IWS conditions. Overall, when the mean saccade amplitude is at 1.2 to 2°, the SHAP value is higher than 0, indicating that the risk of driving would be elevated at this time; when there is IWS, the mean saccade velocity would be centered at 50 to 100°/s, but the effect of the mean saccade velocity on risk elevation or reduction is unclear.

5. Conclusions

(1) As the level of risk increases, there is a downward trend in the mean speed of vehicles. Indicators such as speed SD, acceleration SD, psychophysiological characteristics, and eye movement characteristics all show varying degrees of increase. With the application of IWS, drivers tend to take braking behavior more frequently, increase braking intensity, and decrease vehicle speed. Simultaneously, they reduce the level of tension caused by driving risk, maintain a heightened state of alertness, sustain a wider and more stable saccade amplitude, and increase the saccade velocity.

(2) Compared to SVR and XGBoost, RF has smaller *MAE, MSE*, and *RMSE*, indicating that RF can better express the nonlinear relationship between the IWS, driving behavioral characteristics, and the driving risk and can better analyze the mechanism of different features on driving risk.

(3) The IWS primarily aims to mitigate the level of driving risk by influencing the driver's operation characteristics. When the mean speed, speed SD, acceleration SD, maximum braking depth, mean braking depth, and braking depth SD are within the ranges of 40 to 70 km/h, 3 to 10 km/h, 0 to 0.6 m/s^2, 14 to 16, 0 to 0.2, and 0 to 1, respectively, there is a significant reduction in the degree of risk. Furthermore, the application of the IWS expands the effective range of mean speed and speed SD for reducing driving risk to 40 to 100 km/h and 3 to 15 km/h, respectively.

Data Availability

The authors do not have permission to share data.

Conflicts of Interest

The authors declare that they have no conflicts of interest.

Acknowledgments

This research was funded by Yunnan Fundamental Research Project (Granted No. 202305AC160070 and No. 202201AT070245), Research Projects of Yunnan Transportation Department (Granted No. 2023-83(3)), the General Program of Key Science and Technology in Transportation, the Ministry of Transport (Granted No. 2021-TG-005), Science and Technology Innovation Program of Yunnan Transportation Department (Granted No. Yunjiaokejiaobian [2020]75).

References

[1] X. Liao, Z. Wang, X. Zhao et al., "Cooperative ramp merging design and field implementation: a digital twin approach based on vehicle-to-cloud communication," *IEEE Transactions on Intelligent Transportation Systems*, vol. 23, no. 5, pp. 4490–4500, 2022.

[2] H. Farah, W. Daamen, and S. Hoogendoorn, "How do drivers negotiate horizontal ramp curves in system interchanges in The Netherlands?" *Safety Science*, vol. 119, pp. 58–69, 2019.

[3] J. B. Hu, L. C. He, and R. H. Wang, "Review of safety evaluation of freeway interchange," *China Journal of Highway and Transport*, vol. 33, no. 7, pp. 17–28, 2020.

[4] Y. Yang, N. Tian, Y. Wang, and Z. Yuan, "A parallel FP-growth mining algorithm with load balancing constraints for traffic crash data," *International Journal of Computers, Communications and Control*, vol. 17, no. 4, 2022.

[5] B. Yang, P. Liu, C. Y. Chan, C. Xu, and Y. Guo, "Identifying the crash characteristics on freeway segments based on different ramp influence areas," *Traffic Injury Prevention*, vol. 20, no. 4, pp. 386–391, 2019.

[6] Y. Yang, Y. Yin, Y. Wang, R. Meng, and Z. Yuan, "Modeling of freeway real-time traffic crash risk based on dynamic traffic flow considering temporal effect difference," *Journal of Transportation Engineering, Part A: Systems*, vol. 149, no. 7, 2023.

[7] Y. Zhang and P. A. Ioannou, "Coordinated variable speed limit, ramp metering and lane change control of highway traffic," *IFAC-PapersOnLine*, vol. 50, no. 1, pp. 5307–5312, 2017.

[8] M. U. Megat Johari, N. Megat Johari, T. Savolainen, and J. Gates, "Safety evaluation of freeway exit ramps with advisory speed reductions," *Transportation Research Record: Journal of the Transportation Research Board*, vol. 2677, no. 1, pp. 503–512, 2023.

[9] M. Inoue, K. Baba, and Y. Takada, "Ice detection, prediction, and warning system on highways," *Health Recruitment Board Specification Report*, vol. 115, pp. 17–26, 1970.

[10] S. Mahmud, M. Motz, T. Holpuch et al., "Driver response to a dynamic speed feedback sign on freeway exit ramps based on sign location, interchange type, and time of day," *Transportation Research Record*, vol. 2675, no. 10, pp. 1236–1247, 2021.

[11] S. Mahmud, J. Gates, T. Savolainen, and B. Safaei, "Driver response to a dynamic speed feedback sign at a freeway exit ramp considering the sign design and installation characteristics," *Transportation Research Record: Journal of the Transportation Research Board*, vol. 2677, no. 3, pp. 289–301, 2023.

[12] J. Gates, S. Mahmud, J. Ingle, M. Motz, T. Holpuch, and T. Savolainen, "Evaluation of alternative messages and sign locations on driver response to a dynamic speed feedback sign on a freeway interchange ramp," *Transportation Research Record*, vol. 2674, no. 12, pp. 530–541, 2020.

[13] H. Cui, Z. Wei, X. Wang et al., "Early ramp warning using vehicle behavior analysis," *Soft Computing*, vol. 22, no. 5, pp. 1421–1432, 2018.

[14] X. You, J. Lu, and J. Xue, "Safety early warning and control system of expressway confluence zone based on vehicle-road cooperation," in *2022 14th International Conference on Measuring Technology and Mechatronics Automation (ICMTMA)*, pp. 236–241, IEEE, 2022.

[15] H. Zhou, J. M. Hu, Y. Zhang, and R. Sun, "A coordinated optimization strategy of variable speed limit and ramp metering for expressway," *Journal of Transportation Systems Engineering and Information Technology*, vol. 17, no. 2, p. 68, 2017.

[16] D. Z. Wang, X. H. Song, S. S. Zhu, Y. Chen, and S. Cai, "Merging assistance method based on vehicle-infrastructure cooperative technology," *Journal of Highway and*

Transportation Research and Development, vol. 29, no. S1, pp. 50–56, 2012.

[17] C. Fang, Y. Li, B. Yan, and W. Zhu, "Speed limit model of expressway in rain and fog," *International Conference on Smart Transportation and City Engineering 2021*, vol. 12050, pp. 359–368, 2021.

[18] J. Liu, L. Cai, X. Wang, C. Lyu, and L. Zhang, "Roadside unit deployment of cooperative vehicle-infrastructure system based on digital measurable image method," *Journal of Physics: Conference Series*, vol. 1626, no. 1, p. 012112, 2020.

[19] M. Yang, L. C. Wang, J. Zhang, B. Ran, and J. X. Wu, "Collaborative method of vehicle conflict resolution in merging area for intelligent expressway," *Journal of Traffic and Transportation Engineering*, vol. 20, no. 3, pp. 217–224, 2020.

[20] H. Y. Liu, Z. K. Feng, Y. P. Wu et al.,, "Freeway early warning and emergency avoidance model of the VANET information technology," *Journal of Transportation Systems Engineering and Information Technology*, vol. 18, no. 6, p. 35, 2018.

[21] X. H. Zhao, Y. J. Ju, J. Li et al.,, "Evaluation of the effect of RPMs in extra-long tunnels based on driving behavior and visual characteristics," *China Journal of Highway and Transport*, vol. 33, no. 6, pp. 29–41, 2020.

[22] S. C. Chow, J. Shao, H. Wang, and Y. Lokhnygina, *Sample Size Calculations in Clinical Research*, chapman and hall/CRC, 2017.

[23] Y. Ao, H. Li, L. Zhu, S. Ali, and Z. Yang, "The linear random forest algorithm and its advantages in machine learning assisted logging regression modelling," *Journal of Petroleum Science and Engineering*, vol. 174, pp. 776–789, 2019.

[24] K. Aas, M. Jullum, and A. Løland, "Explaining individual predictions when features are dependent: more accurate approximations to Shapley values," *Artificial Intelligence*, vol. 298, no. 9, pp. 1–23, 2021.